Cerebral blood flow and cerebrovascular reactivity are preserved in a mouse model of cerebral microvascular amyloidosis

Leon P Munting, Marc Pp Derieppe, Ernst Suidgeest, Lydiane Hirschler, Matthias Jp van Osch, Baudouin Denis de Senneville, Louise van Der Weerd

Cerebral blood flow and cerebrovascular reactivity are preserved in a mouse model of cerebral microvascular amyloidosis

Leon P Munting[1,2], Marc PP Derieppe[3], Ernst Suidgeest[1], Lydiane Hirschler[1], Matthias JP van Osch[1], Baudouin Denis de Senneville[4,5], Louise van der Weerd[1,2,*]

[1]Department of Radiology, Leiden University Medical Center, Leiden, the Netherlands.
[2]Department of Human Genetics, Leiden University Medical Center, Leiden, the Netherlands.
[3]Prinses Máxima Center for Pediatric Oncology, University Medical Center Utrecht, Utrecht, the Netherlands.
[4]Department of Radiotherapy, University Medical Center Utrecht, Utrecht, the Netherlands.
[5]Institut de Mathématiques de Bordeaux, Université Bordeaux/CNRS UMR 5251/INRIA, Bordeaux-Sud-Ouest, France.

*Correspondence:
Dr. Louise van der Weerd
P.O. Box 9600, Leiden University Medical Center, Albinusdreef 2, 2300 RC Leiden, the Netherlands
Email: l.van_der_weerd@lumc.nl
Tel: +31 71 526 4760

Running headline: Cerebrovascular function in a model of amyloidosis

ABSTRACT

Impaired cerebrovascular function is an early biomarker for cerebral amyloid angiopathy (CAA), a neurovascular disease leading to stroke and dementia. The transgenic Swedish Dutch Iowa (Tg-SwDI) mouse model is a model for microvascular CAA, but the extent to which the model reflects similar impairments in cerebrovascular function is not yet fully understood. We used arterial spin labeling (ASL)-MRI and laser Doppler flowmetry (LDF) for extensive functional assessment of the Tg-SwDI brain vasculature using a longitudinal study design. Mice were followed-up until 1 year of age, when extensive amyloid-β pathology was visible. Unexpectedly, baseline cerebral blood flow (CBF) and cerebrovascular reactivity (CVR) to a hypercapnia challenge in Tg-SwDI mice showed similar estimates as age-matched wild type control mice. The preserved vascular function was found irrespective of the anesthesia protocol applied, *i.e.*, isoflurane or a combination of urethane and α-chloralose. Changes in CBF and CVR were however observed as an effect of age and anesthesia. Our findings contradict earlier results obtained in the same mouse model and question to what extent microvascular CAA as seen in Tg-SwDI mice is representative for cerebrovascular dysfunction observed in CAA patients.

Key words: arterial spin labeling, cerebral amyloid angiopathy, cerebrovascular function, mouse model, reproducibility

INTRODUCTION

Cerebral amyloid angiopathy (CAA) is a neurovascular disease characterized by accumulation of the amyloid-β peptide in the brain vasculature, which ultimately leads to strokes and cognitive decline.[1] In both hereditary and sporadic variants of CAA, cerebrovascular reactivity (CVR) measurements in patients have shown that impairments in vascular function can be found early in the disease process.[2,3] These measurements were performed with BOLD-fMRI and a visual stimulation paradigm, allowing to characterize CVR in the occipital cortex, where visual processing occurs. The occipital cortex is also where CAA burden is highest,[4] likely contributing to the sensitivity of the fMRI measurement.

Mouse models of cerebral amyloidosis are invaluable tools for testing safety and effectiveness of greatly needed novel therapies for amyloid-β-related diseases, such as CAA. However, for the results to be translatable to the clinic, it is essential that the amyloidosis model shows similar structural and functional phenotypes as the patient. The transgenic Swedish Dutch Iowa (Tg-SwDI) mouse model is an amyloidosis model which expresses low levels of the human amyloid-β precursor protein (APP) gene with 3 familial mutations, of which the Dutch and Iowa mutations are located in the amyloid-β coding region of APP. The neuronal expression of the mutated APP in this model leads to early amyloid-β accumulation in the brain, starting around 6 months. Specifically, the amyloid-β accumulates in the microvasculature, as well as in diffuse amyloid-β plaques in the parenchyma.[5] Previous studies which measured cortical vascular reactivity using laser Doppler flowmetry (LDF) in Tg-SwDI and wild type (WT) mice showed that, similar to patients, Tg-SwDI mice have early impairments in CVR.[6,7] Unlike patients, vascular pathology in this model is most severe in the thalamus,[8] but whether this also leads to increased vascular dysfunction in the thalamus is unknown, as the thalamus is not readily accessible with LDF.

Arterial spin labeling (ASL) is a non-invasive MRI technique in which arterial blood molecules are magnetically labeled and used as endogenous tracer flowing into the tissue of interest, which is most often the brain. The distribution of the label over the different brain regions reflects local tissue perfusion and can be converted into absolute cerebral blood flow (CBF) values, expressed as mL/100 g/min. When combined with a hypercapnic challenge, both CBF and CVR can be determined for different brain regions. A known unfavorable characteristic of ASL is a possible underestimation of CBF in case of slow flow. In that case, a delayed Arterial Transit Time (ATT) – the time that it takes for the label to travel from the labeling plane to the brain tissue – could be misinterpreted as decreased CBF. Measuring ATT could therefore prevent an underestimation of the CBF measurement, as well as be indicative in itself of vascular pathology.[9]

Here, the non-invasive nature of ASL was exploited to study how global and regional CBF and CVR change during increasing amyloid-β accumulation in the brain vasculature of Tg-SwDI mice, using a longitudinal study design. As it is not unlikely that high quantities of microvascular amyloid could lead to delayed ATT in Tg-SwDI mice, ATT was additionally measured with a modified ASL sequence that was optimized to capture the inflow of the tracer into the brain.[10] To allow for repeated measurements, a minimally invasive isoflurane anesthesia protocol was used. However, to be able to compare the results to literature, additional end-point measurements were performed under a terminal anesthesia protocol with urethane and α-chloralose (U&A). Furthermore, a subgroup of mice was used to directly compare ASL-MRI to LDF.

MATERIALS & METHODS

Animals

All the experiments were approved by the local ethics committee ("Leiden University Medical Center Instantie voor Dierenwelzijn") and the national ethical committees ("Centrale Commissie Dierproeven") under OZP PE.18.029.002 of AVD116002017859, and the experiments have been reported in compliance with the ARRIVE guidelines.[11]

Two cohorts of homozygous Tg-SwDI mice and age- and gender-matched WT controls on a C57Bl/6J background were ordered from the Jackson Laboratory (Bar Harbor, ME, USA). The first cohort was followed longitudinally and consisted of 9 male WT mice and 9 male Tg-SwDI mice which were imaged at 3, 6, 9, 12, and 12.3 months of age. The second cohort consisted of 4 Tg-SwDI (2 females) and 4 WT mice (2 females) and was imaged at 8 months of age. Two of the transgenic mice were taken out of the longitudinal study, which was not related to the study itself: the first mouse had to be taken out because it was severely wounded by a cage mate (at 2.5 months of age), the other due to ulcerative dermatitis (at 10 months of age). The mice in the longitudinal cohort were initially co-housed, however, after the aggression incident at 2.5 months, all mice were housed individually to prevent further aggression and to keep the conditions between the mice comparable. Two study-related dropouts occurred in the second cohort (1 wild type and 1 transgenic), due to failure of the intubation procedure (see below). Housing consisted of individually ventilated cages in rooms with a 12-hour day/night rhythm. The cages were supplied with cage bedding, cage enrichment (a small roll to hide in and a block of wood), and unlimited chow food and water.

In vivo Cerebral Blood Flow (CBF) measurements

Mice in the first cohort underwent 5 MRI sessions during which CBF and CVR were measured. To allow for repeated measurements, the first 4 of those measurements were performed under isoflurane. The last measurement was performed under urethane and alpha-chloralose (U&A) for comparability with

literature studies. In the second cohort, there was only one imaging session under U&A anesthesia during which CVR was measured twice, first with Laser Doppler Flowmetry (LDF), and directly thereafter with MRI, to be able to compare both imaging modalities. The study design is summarized in figure 1.

Animal preparation – the isoflurane anesthesia protocol during the first 4 imaging sessions in cohort 1 was similar to the "low isoflurane protocol" as described in Munting *et al.*, 2019.[12] In this protocol, the isoflurane concentration is kept low both during induction (2.0 % for 5 minutes) and maintenance (1.25 %), to limit the vasodilatory effects of the anesthetic. The mouse is freely breathing during the scan. During the 5th imaging session, anesthesia was maintained using 750 mg/kg urethane and 50 mg/kg alpha-chloralose (U&A), similar to the concentrations used by Park *et al.*, 2014.[7] Anesthesia induction with U&A was performed using isoflurane (3.5 %), which was thereafter decreased to 1.75 %. Then, the trachea of the animal was surgically intubated for mechanical ventilation at 80 bpm, 25 % inspiration rate and 1.7 psi (MRI-1 ventilator, CWE Inc., USA). Additionally, an i.p. catheter was placed to administer U&A anesthesia during the MRI scans. Thirty-five minutes after U&A injection, the isoflurane was decreased over the course of 10 minutes to 0 %. During all sessions, transcutaneous partial pressure of carbon dioxide (tc-pCO_2) was monitored (TCM Radiometer, Denmark) with a neonate probe attached to the previously shaved skin on the right flank of the mouse.[13] Breathing rates were monitored using a pressure-sensitive pad placed below the animal (SA Instruments, NY, USA). Temperature was maintained at 36.5 ˚C using a feedback-controlled waterbed with rectal probe (Medres, Germany) and the head was stabilized with a bite bar and ear bars.

The second cohort was also anesthetized with U&A, however, in this cohort, the i.p. injection was given directly after the induction with 3.5 % isoflurane. Again, isoflurane was kept at 1.75 % for 35 minutes after injection, after which it was decreased to 0 % over the course of 10 minutes. While still at 1.75 %

isoflurane, the trachea was surgically intubated for mechanical ventilation and additionally, a craniotomy of 3 mm in diameter was prepared over the right somatosensory cortex. The dura mater was left intact and kept moist with sterile PBS. Similar physiological monitoring was performed as in the first cohort. Fifteen minutes after the isoflurane reached 0 %, the LDF recording was started. After the LDF measurement, and before the animal was placed in the MRI scanner, the skin was placed back over the exposed skull and brain and sutured to limit susceptibility artefacts.

MRI acquisition – a 7 T Pharmascan MRI scanner (Bruker, Germany) with a 23 mm transmit-receive volume coil was used. After proper placement of the mouse head in the bore was confirmed with a scout scan, 3 standard Bruker T2-weighted RARE scans (TE/TR = 35.0 ms/2500 ms; 78 μm^2 resolution) were performed in all 3 directions for consistent planning across animals of the subsequent pseudo-continuous ASL (pCASL) scans. The pCASL scan protocol was similar as in Munting *et al.*, 2019.[12] In short, the phase of the pCASL labeling was first optimized using pre-scans.[14] Thereafter, CBF and CVR were measured using a 21 minute pCASL scan with 180 dynamics, a labeling duration (τ) of 3000 ms, a post-labeling delay (PLD) of 300 ms and a 5 slice spin-echo echo planar imaging (SE-EPI) readout with 225 μm^2 resolution and 1.5 mm slice thickness (no slice gap). 7.5 % CO_2 was administered to the mouse from minute 7 till minute 14. For the fifth time point (12.3 months) of the mice in the first cohort, the number of dynamics of the pCASL scan was extended to 767 (scan duration of 90 minutes) to also capture the effect of switching from isoflurane to U&A anesthesia on CBF. Specifically, the following steps were performed during the 1.5-hour ASL scan: at 5 minutes, U&A was injected, between minutes 40-50 isoflurane was decreased from 1.75 % till 0 % and between minute 72-79, 7.5 % CO_2 was administered. At the fourth scan session (12 months), two time-encoded pCASL (te-pCASL) sequences were additionally acquired per mouse for measuring the ATT. The second te-pCASL sequence was performed

while administering 7.5 % CO_2 to the mouse, which allowed to measure the effect of arterial pCO_2 elevation on the ATT. The scan parameters of the te-pCASL sequence were the same as in Hirschler *et al.*, 2018,[10] except for the resolution, which was decreased from 225 to 337 μm^2 to increase the signal-to-noise ratio (SNR). A 3 slice SE-EPI readout was used, with the same slice orientation as slice 1, 3 and 5 of the standard pCASL scan (thus with a slice gap of 1.5 mm). During every imaging session, for CBF quantification purposes, the T_1 of the tissue (T_{1t}) and the tissue magnetization (M_{0t}) were estimated by collecting an additional inversion recovery scan with the same 5 slice SE-EPI readout as the pCASL scans. Furthermore, a pCASL flow-compensated FLASH was acquired at the level of the carotids, 3 mm downstream of the labeling plane, to measure the labeling efficiency (α). An additional T_2-weighted (T2W) RARE anatomical sequence was acquired with the same slice orientation as that of the pCASL scan for registration purposes.

LDF acquisition – A PeriFlux system with a PF 5010 LDPM unit and two Laser Doppler probes was used for LDF monitoring (Perimed Instruments, Sweden). Both probes were placed at the somatosensory cortex, one directly on the exposed skull above the left hemisphere, the other approximately 0.5 mm above the exposed brain tissue of the right hemisphere (hereafter referred to as the left and right probe, respectively). Extraction of the LDF signal profile was done through DASYLab software (version 13, National Instruments, Germany).

After the last MRI measurement, a subgroup of mice (6 Tg-SwDI and 6 WT) was i.v. injected with 200 µL of DyLight-594-coupled lectin (lycopersicum esculentum, VectorLabs, CA, USA) in the tail vein for staining of the endothelium. This was followed 3 minutes later by an i.p. overdose of pentobarbital after which the mouse was transcardially perfused with 20 mL of ice-cold PBS and 20 mL of ice-cold 4 % PFA. The brain was isolated and overnight fixed in 4 % PFA. The tissue was thereafter preserved at 4 ˚C in PBS

with 0.02 % sodium azide until further processing. The other mice followed the exact same steps, but without the i.v. lectin injection.

Image processing

MR image processing - The image processing pipeline was the same as used in Munting *et al.*, 2019.[12] In short, the SE-EPI frames within one pCASL scan were aligned using the image processing toolbox of MATLAB (version 2018b, Mathworks, USA). Subsequently CBF, CVR and ATT were calculated using the MATLAB based "Multi-Image Analysis (MIA)" software developed at the Grenoble Institute of Neuroscience (Grenoble, France). CBF was expressed in mL/100 g/min, and derived using Buxton's general kinetic perfusion model,[15] with the following equation:

$$\mathrm{CBF} = \frac{\lambda \cdot \Delta M \cdot \exp(\mathrm{PLD}/T_{1b})}{2 \cdot \alpha \cdot T_{1t} \cdot M_{0t} \cdot \left(1 - \exp(-\tau/T_{1t})\right)}$$

where λ is the blood-brain partition coefficient, *i.e.* 0.9 mL/g,[16] ΔM is the signal difference of the label and control images from the standard pCASL scans and T_{1b} is the longitudinal relaxation time of blood, *i.e.* 2230 ms at 7 T.[17] CVR was defined as the average of the last 20 repetitions (≈ 2.3 minutes) during CO_2, over the average of the last 20 repetitions before CO_2 administration. To calculate ATT, the decoded signal from the te-pCASL scans was used, as described in Hirschler *et al.*, 2018.[10] Brain regions of interest (ROIs) were manually drawn on one of the T2W RARE scans, after which they were propagated to the T2W RARE scans of the other datasets (both other mice and other time-points) using the EVolution algorithm.[18] This image registration method was also applied to position the ROIs in the corresponding SE-EPIs. This allowed to retrieve CBF, CVR and ATT values for different brain regions. CBF time-profiles were all filtered using a sliding window of 3 timepoints, besides the profiles acquired in

cohort 2 in the cortical ROI of the hemisphere where the skull was removed (supplementary figure 5), which were filtered with a sliding window of 7 timepoints.

LDF processing - The LDF signal time profiles extracted with DasyLab were filtered with a sliding window of 3 timepoints and normalized to the average signal during the first 7 minutes of the measurement (baseline signal).

Immunohistochemistry (IHC)

The fixed brains were embedded in paraffin, and subsequently cut in sections of 5 µm. After deparaffinization with xylene and rehydration through graded ethanol series, the slides were cooked for 20 minutes in citrate buffer for antigen retrieval. Slides were then stained overnight at 4 °C with anti-amyloid-β antibody (1:1000; Abcam ab2539) followed by a one-hour room temperature incubation with biotinylated secondary antibody (1:300; Dako E0431). Immunodetection was visualized using an Avidin-Biotin Complex kit (Vector Laboratories, UK), and sections were counterstained with haematoxylin before mounting. The slides were digitized with an automatic bright field microscope (Philips Ultra Fast Scanner, Philips, the Netherlands) and assessed by one examiner (LPM) for positivity for amyloid-β.

Statistical testing

To test the effect of genotype on CBF, CVR, ATT, and tc-pCO_2, Mann-Whitney U tests were performed. For the longitudinal cohort, Friedman tests were performed to test the effect of age on CBF and CVR, post-hoc followed by Wilcoxon signed-rank tests to determine which of the individual age groups differed from each other. Only consecutive age-groups were compared to each other to restrict the stringency of the Bonferroni correction for multiple comparisons. Wilcoxon signed-rank tests were used

to test the effect of anesthesia on CBF and CVR and to test the effect of CO_2 on the ATT. No statistical testing was performed in cohort 2, given the small group size. All tests were performed in the SPSS statistics software package, version 26 (IBM, Armonk, NY, USA).

RESULTS

Hypercapnia repeatedly induced a CBF increase in both WT and Tg-SwDI mice in the longitudinal cohort (figure 2a), which was mainly located in cortical regions (figure 2b). Surprisingly, the CBF time-profiles of the Tg-SwDI mice resembled those of the WT mice at every time-point. Hence no significant differences were observed in baseline CBF nor CVR between the two genotypes at any time-point (figure 3; see supplementary figure 1 for individual animal trends). A significant effect of age on CBF was however observed in both WT and Tg-SwDI mice, $\chi^2(3) = 13.00$, $p = 0.005$ and $\chi^2(3) = 8.49$, $p = 0.037$, respectively. Post-hoc analysis indicated that this was attributable to a decrease in baseline CBF between the age of 3 and 6 months. Between these time-points, median (iqr) CBF significantly decreased from 155 (143-159) to 121 (112-124) mL/100 g/min in WT mice, $p = 0.008$. In Tg-SwDI mice, a similar trend was observed, from 147 (133-151) to 126 (103-135) mL/100 g/min, $p = 0.036$, but this was not significant (cut-off p-value of 0.017 after Bonferroni correction). From 6 months of age, the baseline CBF remained stable inside each group. Age also had a significant effect on CVR in WT mice, $\chi^2(3) = 8.33$, $p = 0.040$. No differences were observed with post-hoc analysis however, besides a trend towards increased CVR between the age of 3 and 6 months, from 13 (7-17) to 31 (23-37) %, $p = 0.038$. Age had no significant effect on CVR in Tg-SwDI mice, $\chi^2(3) = 6.94$, $p = 0.074$. Additional analysis in cortical and thalamic areas did not reveal any difference between WT and Tg-SwDI mice either (supplementary figure 2). Similarly, no differences were observed in the tc-pCO_2 upon the hypercapnia challenges between WT and Tg-SwDI mice (supplementary figure 3).

Median (iqr) baseline ATT values were also similar for both WT and Tg-SwDI mice, i.e. 199 (177-227) milliseconds (ms) and 200 (180-213) ms respectively at 12 months of age (figure 4). The hypercapnia challenge significantly shortened the ATT, Z = -2.55 and p = 0.011 for WT mice, Z = -2.37 and p = 0.018 for Tg-SwDI mice, with a similar reduction in both genotypes (about 25 ms).

To evaluate if a functional deficit could have been masked by the isoflurane administration during the MRI sessions, additional CBF and CVR measurements were performed in the same cohort of mice under urethane and alpha-chloralose (U&A) anesthesia. This was done at 12.3 months, 10 days after the last MRI measurement under isoflurane. The change of anesthesia protocol resulted in profound hemodynamic changes: baseline CBF was severely reduced and the response to hypercapnia was much higher but also slower (figure 5a), and much more widespread in the brain tissue (figure 5b). Indeed, CBF and CVR were significantly affected by the change in anesthesia protocol (figure 5c), with the median CBF (iqr) decreasing from 126 (84-141) to 28 (26-30) mL/100 g/min in WT mice, Z = -2.67 and p = 0.008, and median (iqr) CVR increasing from 26 (6-47) to 233 (193-245) %, Z = -2.67 and p = 0.008. These changes were again comparable to those in Tg-SwDI mice, with the median CBF (iqr) and CVR (iqr) respectively changing from 114 (103-130) to 25 (21-40) mL/100 g/min, Z = - 2.37 and p = 0.018, and from 30 (17-34) to 265 (178-312) %, Z = -2.37 and p = 0.018. The higher CVR during U&A was unlikely the result of higher CO_2 absorption, as the tc-pCO_2 responses to the hypercapnia challenges during isoflurane and U&A were comparable (supplementary figure 3). The CBF response to the induction phase of U&A anesthesia was also similar in Tg-SwDI and WT mice (supplementary figure 4).

An additional smaller second cohort of mice was used to directly compare our MRI findings to the previously used LDF technique as imaging modality to assess cerebrovascular function in this mouse model.[6,7] LDF and MRI measurements were performed directly after each other in the same mouse and

the brain region analyzed with the MRI data was restricted to the somatosensory cortex, approximately similar to where the LDF measurement was performed. No differences in CVR could be observed between WT and Tg-SwDI mice, neither with MRI, nor with LDF (figure 6). Of note, removal of the skull severely reduced the CVR for both imaging modalities (supplementary figure 5).

Lastly, tissue was stained for amyloid-β to assess the degree of pathological burden. All the Tg-SwDI mice developed extensive amyloid-β plaque pathology by the end of the experiment, with mainly diffuse parenchymal plaques in the cortex and microvascular plaques in the hippocampus and thalamus, but none of the WT mice did (figure 7).

DISCUSSION

The most prominent finding of this study is that we did not find any impairments in cerebrovascular function in the Tg-SwDI model of CAA, no matter the age or functional measurement studied. This contradicts previous findings, which showed early impairments in the cerebral cortex in Tg-SwDI mice using LDF.[6,7] Here, cerebrovascular function was first assessed using Arterial Spin Labeling (ASL)-MRI and a CO_2 challenge, allowing to measure absolute CBF as well as CVR in the entire brain. The ASL-MRI measurements were acquired longitudinally using the minimally invasive anesthetic isoflurane to capture the dynamics of decreasing cerebrovascular function over increasing microvascular amyloid-β loads. This is substantially different from literature studies, where relative CBF measurements were performed using LDF under a terminal anesthesia protocol with urethane and α-chloralose (U&A) after removal of the skull.[6,7] Therefore, additional experiments were performed to determine whether the differences in experimental design could explain the discrepancy. A likely candidate was the difference in anesthesia, as the type of anesthesia protocol used has been shown to significantly influence CVR experiments.[12,19] Another likely candidate was the difference in imaging modality, as ASL-MRI and LDF

are sensitive to different blood components, namely blood plasma (ASL-MRI) or red blood cells (LDF). However, after differences in anesthesia protocol and imaging modality were accounted for, vascular function was still found to be preserved in our hands in the Tg-SwDI model. Practically, it is very difficult to replicate an experiment up to the smallest detail in a different laboratory, as small differences will always remain. To the best of our knowledge however, the most fundamental differences in the protocols (anesthesia and imaging modality) have been accounted for. Furthermore, changes in CBF and CVR as a result of age and anesthesia were detected, thus demonstrating that we did not lack sensitivity to detect hemodynamic changes. The CBF time-profiles of Tg-SwDI mice were in fact remarkably similar to their wild type controls, even when CBF was monitored up to 1.5 hours (supplementary figure 4). Therefore, the extent to which the Tg-SwDI model can be used in vascular function studies in the context of CAA and novel treatment studies could be questioned.

Some remaining differences between our approach and those of others are however useful to mention and could possibly provide explanations for the different outcomes between the studies. Chow *et al*.,[6] as well as Park *et al*.,[7] used heterozygotic Tg-SwDI mice, whereas here, homozygotic Tg-SwDI mice were used. Homozygotic Tg-SwDI mice have been reported to develop more extensive amyloid-β pathology, but with a similar distribution on the micro- and macro-scale in the brain and similar amyloid-β-40/amyloid-β-42 ratios as hemizygous mice.[20] It seems however unlikely that the more severe pathology would result in a reversal of the functional phenotype. Furthermore, the amyloid-β pathology found here (figure 7) is comparable to what is described in literature for both hemizygous and homozygous mice, namely diffuse parenchymal plaques in the cortex and microvascular accumulation in the thalamus and hippocampus.[8] Secondly, we used a higher percentage of CO_2 for our vascular challenge, *i.e.* 7.5 % for 7 minutes here, versus *vs.* 5 % for 5 minutes in literature.[7] However, it is unlikely

that higher pCO_2 rises would reverse the phenotype of the Tg-SwDI mice. Furthermore, the pCO_2 increase measured here through the skin during U&A is comparable to the increase reported with blood gas sampling in Park *et al.*[7] (approximately 20 mmHg). Possibly, a lower sensitivity of the transcutaneous pCO_2 measurement versus blood gas sampling could explain why our pCO_2 increase is not higher. Lastly, in Chow *et al.*,[6] and Park *et al.*,[7] an acutely prepared craniotomy was performed before the LDF measurement, whereas here, most of the measurements were performed non-invasively. An attempt was made to account for this difference in experimental set-up by preparing an acute craniotomy in the second cohort of mice. However, after the craniotomy, the CVR was nearly abolished in the underlying brain regions in both genotypes and with both imaging modalities. Furthermore, the MRI measurements showed prominent edema in all animals that underwent craniotomy, even though the brain surface in these animals seemed to be normal by eye (supplementary figure 5). The researcher that performed the craniotomy in this study is highly skilled in this procedure, underlining that this effect is not merely a matter of experience. Nevertheless, it could be argued that there must be something in our surgical procedure that makes it more invasive than the protocol of others,[6,7] and thereby reduces CVR in the underlying tissue. It could be further hypothesized that a less invasive craniotomy is in fact a required second hit, after the accumulation of amyloid-β, to evoke vascular dysfunction in Tg-SwDI mice. Recently, a study reported that skull removal was necessary to detect vascular dysfunction in a different mouse model of amyloid-β accumulation, thus supporting this hypothesis.[21] It is of interest to elucidate in in future research how different surgical procedures affect CVR, and whether surgery can evoke vascular dysfunction in Tg-SwDI mice.

Besides the contrasting results on vascular function in Tg-SwDI mice, there are a few other interesting findings in this study. To the best of our knowledge, this is the first study with ASL-MRI in mice where

the CBF responses to hypercapnia under isoflurane or U&A anesthesia are directly compared. Large differences in both parameters were observed, with the very low CBF during U&A anesthesia as the most striking observation. U&A is considered one of the better anesthesia protocols for cerebral hemodynamic studies in mice, as the anesthetics have been reported to have relatively mild effects on hemodynamics[22,23] and to maintain cerebral autoregulation.[24] However, these studies did not quantify CBF absolutely, and our results indicate that the stable hemodynamics come together with very low baseline CBF, which may not always be favorable and certainly do not represent normal baseline physiology. It would be of interest to identify the underlying cause for this low CBF. This is also one of the few studies where a direct comparison was made between hypercapnic CBF responses measured with ASL-MRI versus LDF. The results must however be interpreted with care due to the small group size and the ± 0.5-hour delay between the two measurements. Both measurements consistently reported preservation of vascular function in Tg-SwDI mice and a severe reduction of CVR after craniotomy, but CVR measurements with ASL-MRI were nearly twice as high as those obtained with LDF. It is unclear where this difference comes from. As the two imaging modalities are sensitive to different blood components (plasma or red blood cells), it could be argued that local hematocrit changes during hypercapnia must be underlying this difference. Indeed, hematocrit has been reported to decrease during hypercapnia in the rat brain,[25] but with only a 10 % decrease during a 10 % CO_2 challenge, which is too low to explain the observed difference. A more convincing explanation could be found in an interesting study where ASL-MRI and LDF were used simultaneously,[26] and point in the direction of an underestimation by LDF. The authors showed that by varying the fiber separation distance in the LDF probe, which changes the measured cortical depth, different CBF response were measured. Consequently, the magnitude of the CBF response was either comparable to that measured with ASL-MRI, or up to two times lower, which is comparable to our results. The authors measured CBF

responses to electrical whisker stimulation through a thinned skull in rats under urethane anesthesia, and concluded that when larger cortical depths were measured, LDF underestimated the CBF response. It is unclear how these results would exactly translate to our different set-up (smaller cortical thickness in the mouse, intact skull, different vascular challenge), but indicates that investigating the cortical depth measured with a set-up like ours is a compelling area for future research. Interestingly, the absolute CBF responses measured with ASL-MRI by He *et al.*,[26] were comparable to those measured here. Lastly, another finding in our study that is of interest, is the observation of edema and the local reduction in CBF and CVR with MRI after craniotomy. This was observed in all animals, while the brain tissue seemed normal on visual inspection. Normal appearing brain tissue is therefore not enough to conclude that the brain tissue is healthy when working with acutely prepared cranial windows.

In conclusion, this study shows that cerebrovascular function in the Tg-SwDI mouse model of CAA is preserved up to 12 months of age, despite the high amyloid-β burden observed at that age. This observation was confirmed using two different anesthesia protocols and two different imaging modalities. These observations call into question to what extent microvascular CAA as seen in the Tg-SwDI mouse model is a correct model for vascular dysfunction as observed in CAA patients, and calls for further research to clear up the discrepancy in results.

ACKNOWLEDGEMENTS

The authors would like to thank the following persons: Thas Phisonkunkasem, Nico Jansen, Maarten Schenke and Else Tolner for their help with setting up the LDF measurements, Laibaik Park for his advice on the urethane and α-chloralose anesthesia protocol, and Ingrid Hegemann-Klein and Marjolein Bulk for their help with the histology. L. van der Weerd, M.P.P. Derieppe and L.P. Munting are supported by the Netherlands Organization for Scientific Research (NWO) Innovational Research Incentives Scheme

(VIDI grant 864.13.014) and the CVON heart-brain axis connection of the Dutch heart society. M.J.P. van Osch and L. Hirschler are supported by the Division Applied and Engineering Sciences of the NWO (VICI grant 016.160.351).

AUTHOR CONTRIBUTION STATEMENT

LPM contributed to experimental design, data acquisition, image processing, data analysis, and manuscript preparation; MPPD contributed to image processing, data analysis and manuscript preparation; ES contributed to data acquisition; LH contributed to image processing; MJPO contributed to experimental design and manuscript preparation; BDS contributed to image processing; LW contributed to experimental design and manuscript preparation.

DISCLOSURE/CONFLICT OF INTEREST

The authors declare that there is no conflict of interest.

SUPPLEMENTARY INFORMATION

Supplemental material for this article is available online.

REFERENCES

1. Banerjee G, Carare R, Cordonnier C, et al. The increasing impact of cerebral amyloid angiopathy: Essential new insights for clinical practice. *Journal of Neurology, Neurosurgery and Psychiatry* 2017; 88: 982–994.

2. Dumas A, Dierksen GA, Gurol ME, et al. Functional magnetic resonance imaging detection of vascular reactivity in cerebral amyloid angiopathy. *Ann Neurol* 2012; 72: 76–81.

3. van Opstal AM, van Rooden S, van Harten T, et al. Cerebrovascular function in presymptomatic and symptomatic individuals with hereditary cerebral amyloid angiopathy: a case-control study. *Lancet Neurol* 2017; 16: 115–122.

4. Yamada M, Tsukagoshi H, Otomo E, et al. Cerebral amyloid angiopathy in the aged. *J Neurol* 1987; 234: 371–376.

5. Davis J, Xu F, Deane R, et al. Early-onset and Robust Cerebral Microvascular Accumulation of Amyloid β-Protein in Transgenic Mice Expressing Low Levels of a Vasculotropic Dutch/Iowa Mutant Form of Amyloid β-Protein Precursor. *J Biol Chem* 2004; 279: 20296–20306.

6. Chow N, Bell RD, Deane R, et al. Serum response factor and myocardin mediate arterial hypercontractility and cerebral blood flow dysregulation in Alzheimer's phenotype. *Proc Natl Acad Sci U S A* 2007; 104: 823–828.

7. Park L, Koizumi K, El Jamal S, et al. Age-dependent neurovascular dysfunction and damage in a mouse model of cerebral amyloid angiopathy. *Stroke* 2014; 45: 1815–1821.

8. Miao J, Xu F, Davis J, et al. Cerebral Microvascular Amyloid β Protein Deposition Induces

Vascular Degeneration and Neuroinflammation in Transgenic Mice Expressing Human Vasculotropic Mutant Amyloid β Precursor Protein. *Am J Pathol* 2005; 167: 505–515.

9. Alsop DC, Detre JA, Golay X, et al. Recommended implementation of arterial spin-labeled perfusion MRI for clinical applications: A consensus of the ISMRM perfusion study group and the European consortium for ASL in dementia. *Magn Reson Med*. Epub ahead of print 8 April 2014. DOI: 10.1002/mrm.25197.

10. Hirschler L, Munting LP, Khmelinskii A, et al. Transit time mapping in the mouse brain using time-encoded pCASL. *NMR Biomed* 2018; 31: e3855.

11. Kilkenny C, Browne WJ, Cuthill IC, et al. Improving Bioscience Research Reporting: The ARRIVE Guidelines for Reporting Animal Research. *PLoS Biol* 2010; 8: e1000412.

12. Munting LP, Derieppe MPP, Suidgeest E, et al. Influence of different isoflurane anesthesia protocols on murine cerebral hemodynamics measured with pseudo-continuous arterial spin labeling. *NMR Biomed*; 32. Epub ahead of print 1 August 2019. DOI: 10.1002/nbm.4105.

13. Ramos-Cabrer P, Weber R, Wiedermann D, et al. Continuous noninvasive monitoring of transcutaneous blood gases for a stable and persistent BOLD contrast in fMRI studies in the rat. *NMR Biomed* 2005; 18: 440–6.

14. Hirschler L, Debacker CS, Voiron J, et al. Interpulse phase corrections for unbalanced pseudo-continuous arterial spin labeling at high magnetic field. *Magn Reson Med* 2018; 79: 1314–1324.

15. Buxton RB, Frank LR, Wong EC, et al. A general kinetic model for quantitative perfusion imaging with arterial spin labeling. *Magn Reson Med* 1998; 40: 383–96.

16. Herscovitch P, Raichle ME. What is the correct value for the brain--blood partition coefficient for water? *J Cereb Blood Flow Metab* 1985; 5: 65–69.

17. Dobre MC, Uğurbil K, Marjanska M. Determination of blood longitudinal relaxation time (T1) at high magnetic field strengths. *Magn Reson Imaging* 2007; 25: 733–735.

18. Denis de Senneville B, Zachiu C, Ries M, et al. EVolution: an edge-based variational method for non-rigid multi-modal image registration. *Phys Med Biol* 2016; 61: 7377–7396.

19. Petrinovic MM, Hankov G, Schroeter A, et al. A novel anesthesia regime enables neurofunctional studies and imaging genetics across mouse strains. *Sci Rep* 2016; 6: 24523.

20. Xu F, Grande AM, Robinson JK, et al. Early-onset subicular microvascular amyloid and neuroinflammation correlate with behavioral deficits in vasculotropic mutant amyloid β-protein precursor transgenic mice. *Neuroscience* 2007; 146: 98–107.

21. Sharp PS, Ameen-Ali KE, Boorman L, et al. Neurovascular coupling preserved in a chronic mouse model of Alzheimer's disease: Methodology is critical. *J Cereb Blood Flow Metab* 2019; 271678X19890830.

22. Janssen BJA, De Celle T, Debets JJM, et al. Effects of anesthetics on systemic hemodynamics in mice. *Am J Physiol - Hear Circ Physiol*; 287. Epub ahead of print October 2004. DOI: 10.1152/ajpheart.01192.2003.

23. Wang Z, Schuler B, Vogel O, et al. What is the optimal anesthetic protocol for measurements of cerebral autoregulation in spontaneously breathing mice? *Exp Brain Res* 2010; 207: 249–258.

24. Dalkara T, Irikura K, Huang Z, et al. Cerebrovascular responses under controlled and monitored

physiological conditions in the anesthetized mouse. *J Cereb Blood Flow Metab* 1995; 15: 631–8.

25. Keyeux A, Ochrymowicz-Bemelmans D, Charlier AA. Induced response to hypercapnia in the two-compartment total cerebral blood volume: Influence on brain vascular reserve and flow efficiency. *J Cereb Blood Flow Metab* 1995; 15: 1121–1131.

26. He J, Devonshire IM, Mayhew JEW, et al. Simultaneous laser Doppler flowmetry and arterial spin labeling MRI for measurement of functional perfusion changes in the cortex. *Neuroimage* 2007; 34: 1391–1404.

FIGURE CAPTIONS

Figure 1: Study design. Two different cohorts were used in this study, of which the first was followed longitudinally. The timeline of the first cohort is illustrated in the upper part of the figure, with scan moments indicated with orthogonal arrows projected onto the timeline. The most relevant scans performed at these moments are indicated within the boxes adjoined to the orthogonal arrows and the type of anesthesia used is indicated in *italic* on top of the boxes. The lower part of the figure illustrates the single timepoint measurements performed in cohort 2.
pCASL = pseudo-continous arterial spin labeling; te-p. = time-encoded pseudo-continous arterial spin labeling; U&A = urethane and α-chloralose; LDF = laser Doppler flowmetry

Figure 2: Cerebral blood flow (CBF) time-profiles and CBF maps in wild type (WT) and transgenic Swedish Dutch Iowa (Tg-SwDI) mice. A) displays 21-minute CBF time-profiles (mean ± standard deviation) that were acquired at the ages of 3,6,9 and 12 months old in the longitudinal cohort.

CO_2 was administered between minute 7 and 14. B) displays MR images acquired in the mid-brain in representative 9-months old WT (top row) and Tg-SwDI mice (bottom row). In the columns from left to right are displayed: anatomical T_2-weighted images, baseline CBF maps, CBF maps acquired during CO_2 administration and cerebrovascular reactivity (CVR) maps.

Figure 3: Boxplot representation of the baseline cerebral blood flow (CBF) and cerebrovascular reactivity (CVR) values acquired in the longitudinal cohort. Given are the measurements acquired in 3,6,9 and 12-months old wild type and transgenic Swedish Dutch Iowa (Tg-SwDI) mice, where circles and squares represent individual mice. No significant differences were observed between the two genotypes, but there was a significant effect of age ($p = 0.005$ for CBF in WT, $p = 0.037$ for CBF in TG, $p = 0.040$ for CVR in WT). From the post-hoc analysis, only the drop in CBF in WT mice between 3 and 6 months old reached the Bonferroni-corrected significance threshold ($p = 0.008$).

Figure 4: Arterial Transit Time (ATT) measurements acquired in 12-months old wild type (WT) and transgenic Swedish Dutch Iowa (Tg-SwDI) mice. On the top row, measurements acquired at baseline are displayed, on the bottom row measurements acquired while administering 7.5 % CO_2. On the left column, graphs display the measured arterial spin labeling (ASL) signal (mean ± standard deviation) plotted against increasing post-label delay times. In the middle, maps are displayed that show arrival times of the ASL signal in different brain regions. The maps were acquired in a posterior brain slice of a representative WT mouse (top) or Tg-SwDI mouse (bottom). On the right, boxplot representations of the ATT values obtained in all mice are displayed, where circles and squares represent individual mice.

Figure 5: Cerebral blood flow (CBF) and cerebrovascular reactivity (CVR) acquired during isoflurane

anesthesia and urethane & α-chloralose (U&A) anesthesia. A) displays 21-minute CBF time-profiles acquired in wild type (WT) and transgenic Swedish Dutch Iowa (Tg-SwDI) mice under either isoflurane anesthesia (left, 12 months old) or U&A anesthesia (right, 10 days later). CO_2 was administered between minute 7 and 14. B) displays representative CBF and CVR maps acquired in a representative WT (top) or Tg-SwDI (bottom) mouse. All 6 images on one row are acquired in the same mouse. C) displays boxplot representations of the baseline CBF and CVR group values, where dots and circles represent individual mice.

Figure 6: Cerebral blood flow (CBF) time-profiles acquired with laser Doppler flowmetry (LDF) and Arterial Spin Labeling (ASL)-MRI. On the left, 21-minute CBF time-profiles acquired with LDF in the somatosensory cortex are displayed for wild type (WT) and transgenic Swedish Dutch Iowa (Tg-SwDI) mice. In the middle, 21-minute CBF time-profiles are displayed that are acquired with ASL-MRI in the left somatosensory cortex, after baseline correction, so the profiles can be compared to the LDF time-profiles. On the right are the same profiles as in the middle, without baseline correction.

Figure 7: Amyloid-β histology in representative wild type (WT) and transgenic Swedish Dutch Iowa (Tg-SwDI) mice of 12.3 months old. The upper row is an overview image, the other rows are zoomed in regions from the overview image.

Supplementary figure 1: Animal-by-animal CBF and CVR progression with increasing age. On the top row, CBF trends are displayed, on the bottom row CVR trends. The left column shows wild type (WT) mice, the right column transgenic Swedish Dutch Iowa (Tg-SwDI) mice.

Supplementary figure 2: Cerebral blood flow (CBF) measurements in cortical (left) and thalamic (right)

ROIs. On the top row, representative T_2-weighted images are shown with overlaying areas (in gray) representing the brain regions that were analyzed. The middle row shows CBF time-profiles (mean ± standard deviation) acquired in these brain regions. The bottom row shows boxplot representations of the CBF and cerebrovascular reactivity (CVR) from the same brain regions. Dots and circles represent individual mice.

Supplementary figure 3: Change in transcutaneously measured pCO_2 during the hypercapnia challenges. Displayed are pCO_2 time-profiles (mean ± standard deviation) acquired during the first hypercapnia challenge of the different timepoints of cohort 1.

Supplementary figure 4: CBF change observed during switching from isoflurane anesthesia to urethane and α-chloralose (U&A). 90-minute CBF time-profiles (mean ± standard deviation) are displayed acquired in cohort 1 at an age of 12.3 months old. U&A was injected 5 minutes after the start of the arterial spin labeling-MRI scan. Isoflurane (iso) was decreased between minute 40 and 50. CO_2 was administered between minute 72 and 79.

Supplementary figure 5: Cerebrovascular reactivity (CVR) measurements with Laser Doppler flowmetry (LDF) and arterial spin labeling (ASL-MRI) with and without skull removal. A) displays CVR time-profiles acquired either with LDF (top row) or ASL-MRI (bottom row). The left column shows the CVR time-profiles from the intact, left hemisphere, the right column the profiles from the right hemisphere after craniotomy. B) shows a photograph of the somatosensory cortex of a representative mouse after craniotomy on the top row, and on the bottom row, the T_2-weighted, cerebral blood flow (CBF) and CVR images that were acquired with MRI after craniotomy. Note that the left hemisphere is displayed on the right, according to radiological convention.

Cohort 1 - Longitudinal

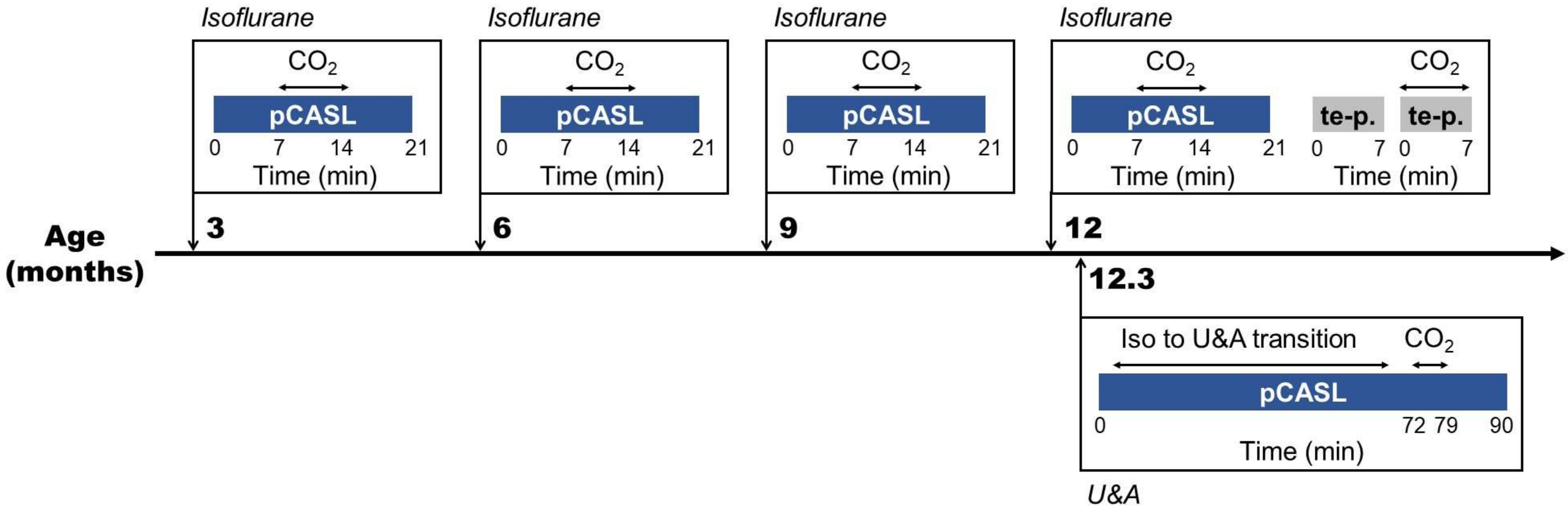

Cohort 2 – Single timepoint

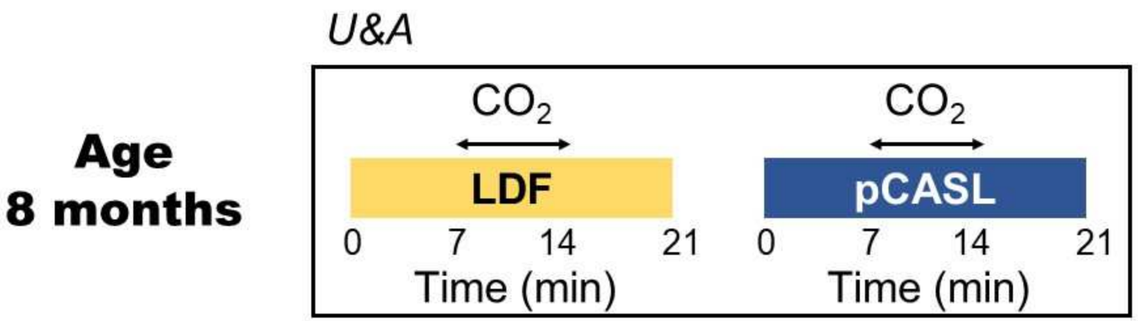

A)

3 Months

6 Months

9 Months

12 Months

CBF (mL/100 g/min)

200
180
160
140
120
100
80

0
7
14
21

7.5 % CO_2

Wild type
Tg-SwDI

Time (minutes)

B)

CBF baseline
(mL/100 g/min)

CBF during CO_2
(mL/100 g/min)

CVR
(%)

WT

Tg

0
220

0
220

-40
80

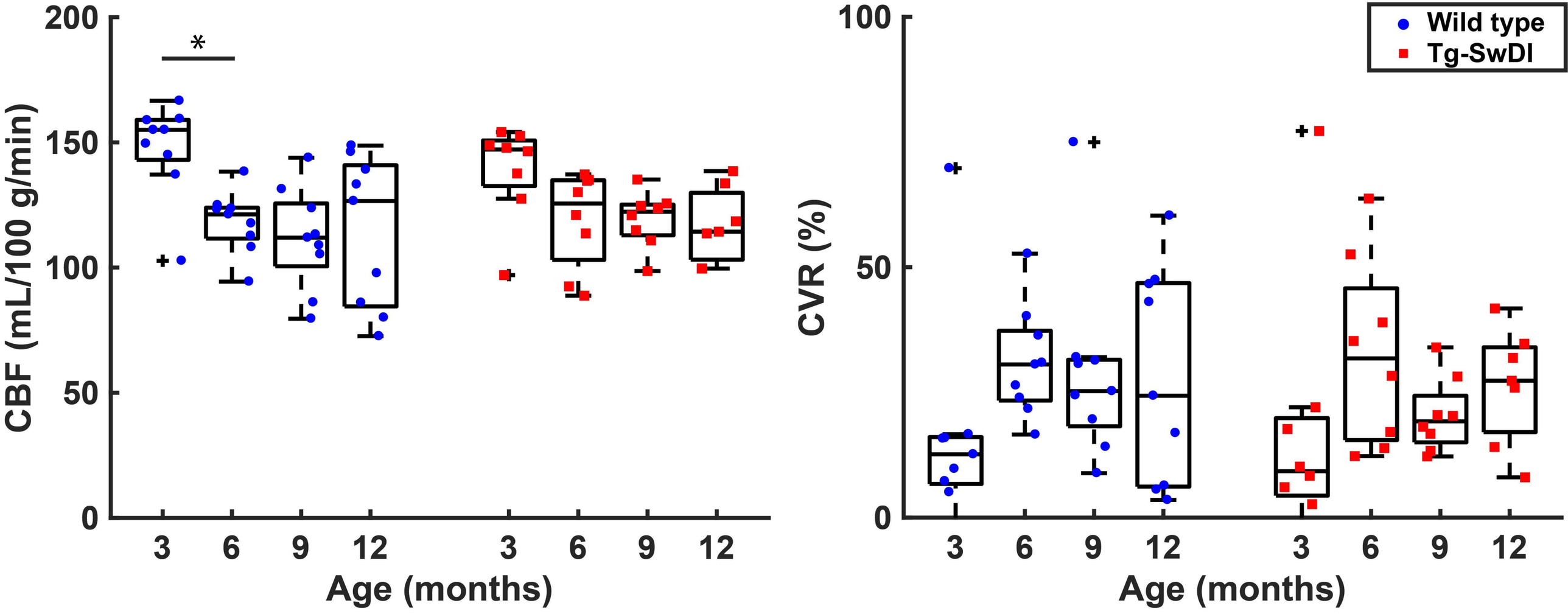
CBF (mL/100 g/min)
200
150
100
50
0
*
3
6
9
12
3
6
9
12
Age (months)
CVR (%)
100
50
0
Wild type
Tg-SwDI
3
6
9
12
3
6
9
12
Age (months)

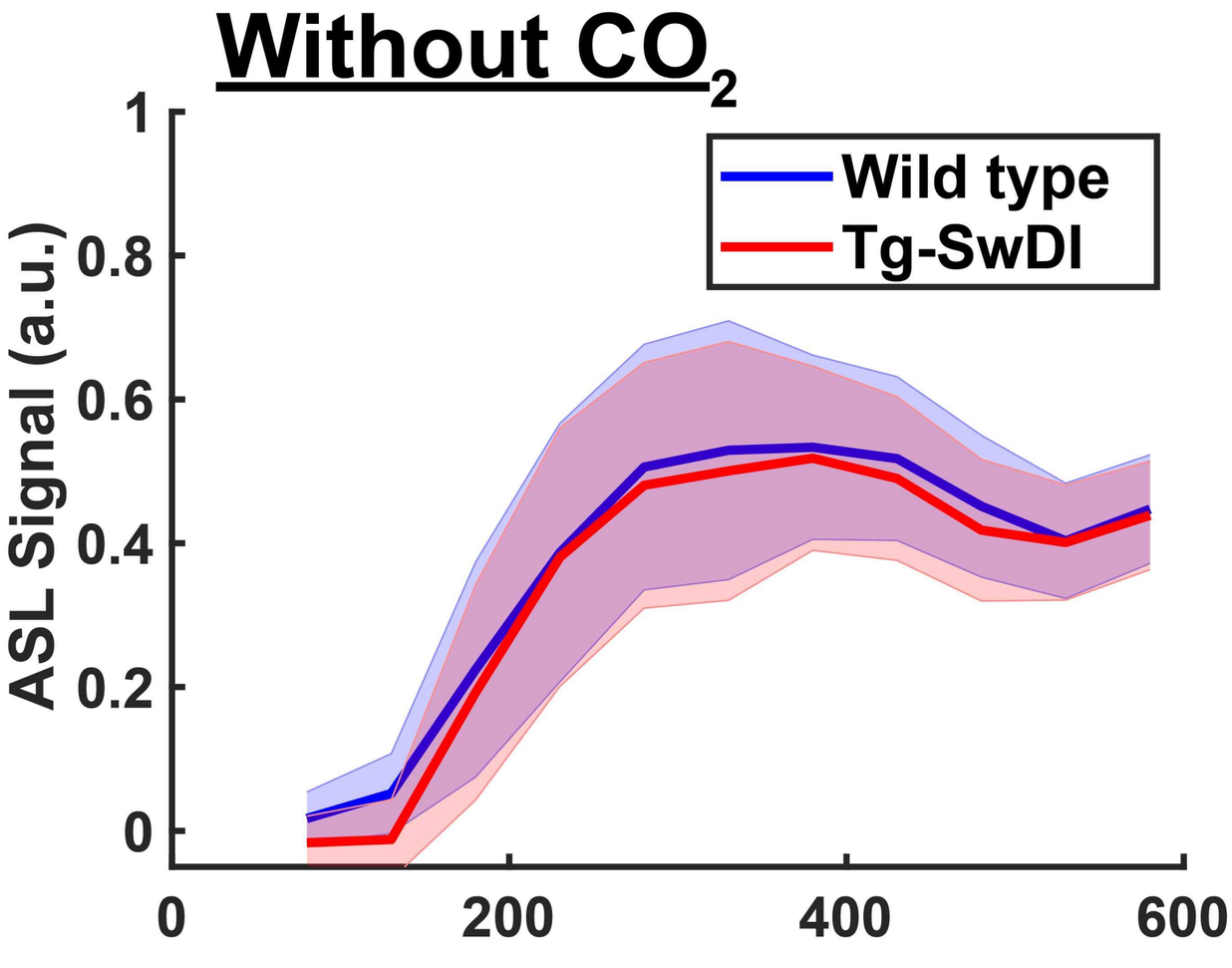
Without CO_2
Wild type
Tg-SwDI
ASL Signal (a.u.)
0
0.2
0.4
0.6
0.8
1
0
200
400
600

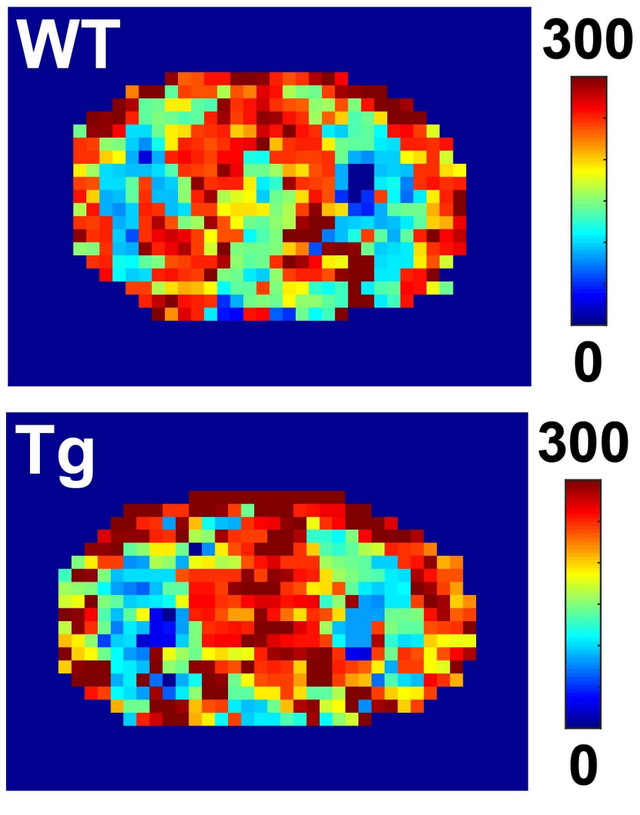
WT
300
0
Tg
300
0

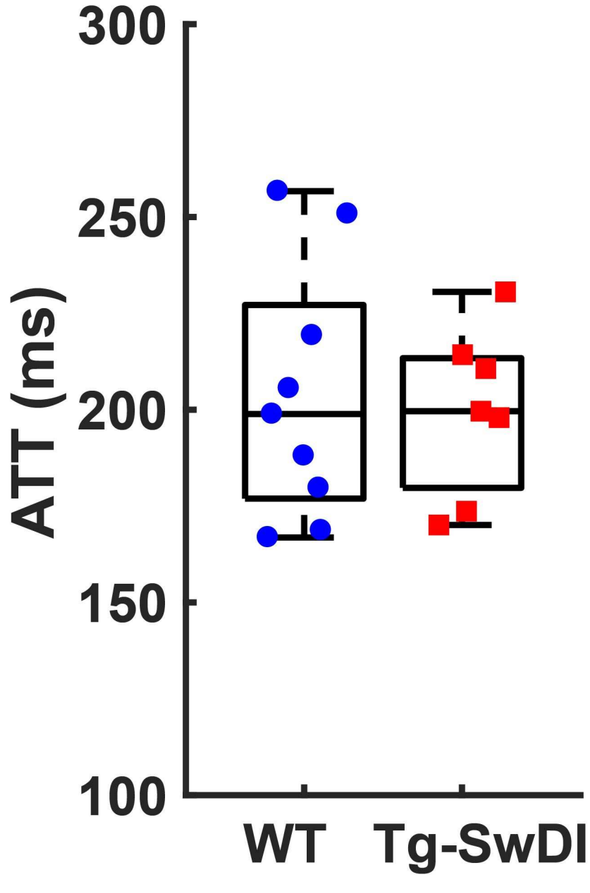
ATT (ms)
300
250
200
150
100
WT
Tg-SwDI

With CO_2
ASL Signal (a.u.)
0
0.2
0.4
0.6
0.8
1
0
200
400
600
Time (ms)

WT
300
0
Tg
300
0
ATT (ms)

ATT (ms)
300
250
200
150
100
WT
Tg-SwDI

A)

Isoflurane

Urethane & α-chloralose

CBF (mL/100 g/min)

180
150
120
90
60
30
0

7.5 % CO_2

Wild type
Tg-SwDI

0 7 14 21

Time (minutes)

B)

CBF baseline (mL/100 g/min)

CBF with CO_2 (mL/100 g/min)

CVR (%)

WT

Tg

0 250

0 250

-40 80

0 250

0 250

-40 400

C)

CBF (mL/100 g/min)

200
150
100
50
0

WT Tg-SwDI

CVR (%)

400
300
200
100
0

WT Tg-SwDI

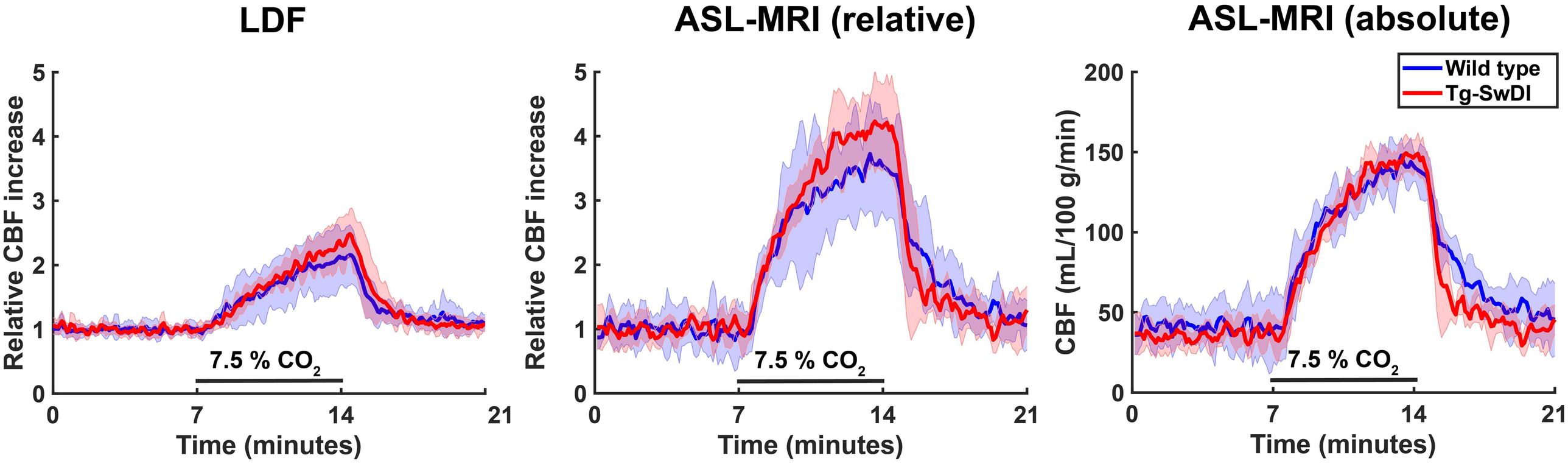
LDF
ASL-MRI (relative)
ASL-MRI (absolute)
Relative CBF increase
CBF (mL/100 g/min)
Time (minutes)
7.5 % CO2
Wild type
Tg-SwDI
0
1
2
3
4
5
50
100
150
200
7
14
21

Wild type

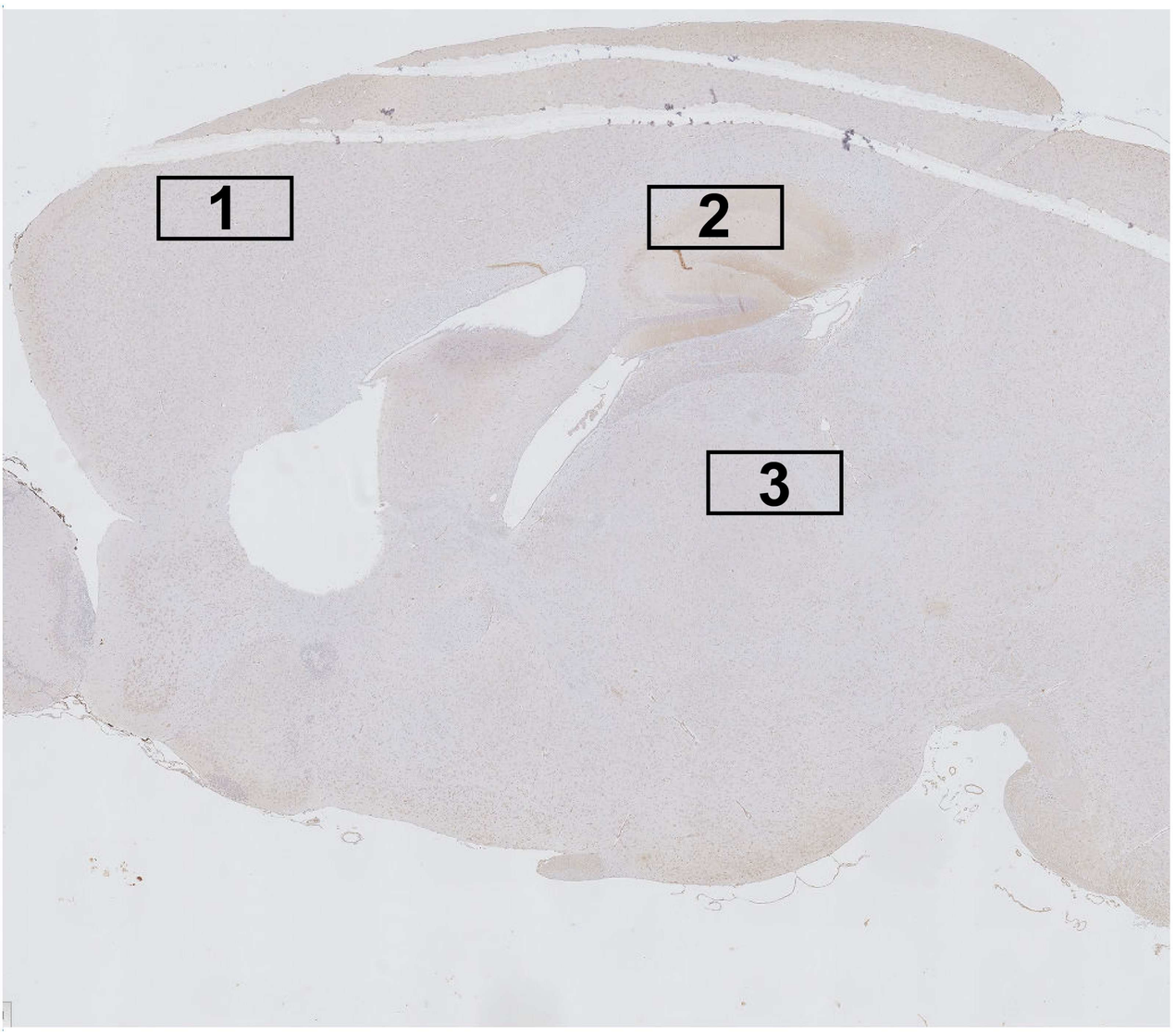

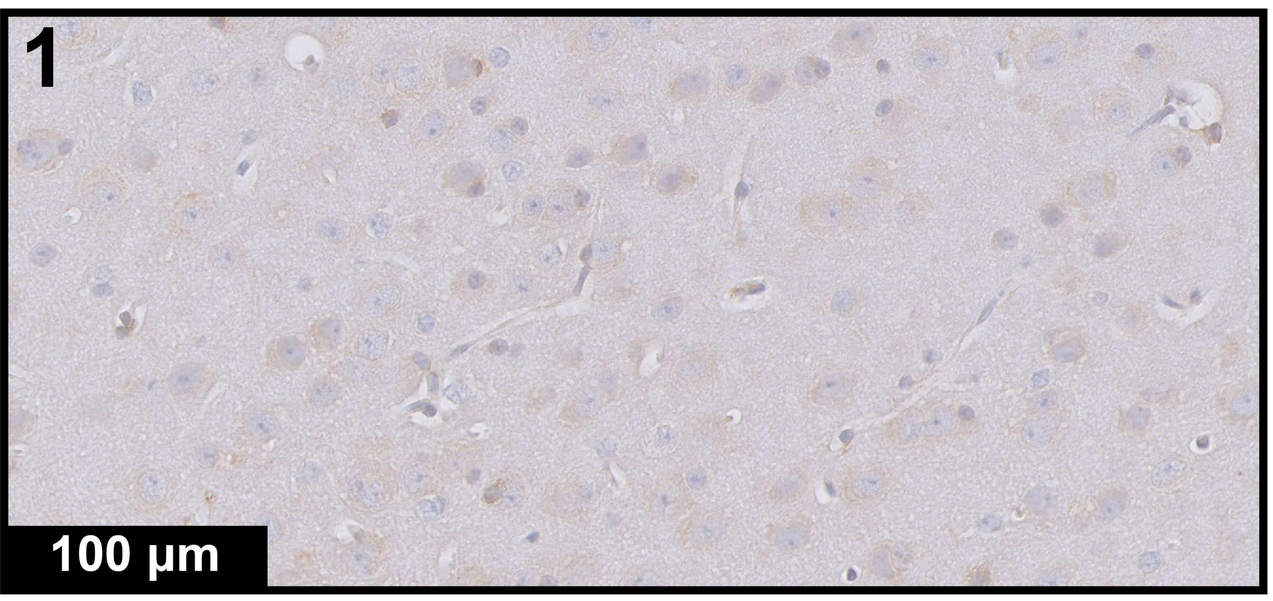

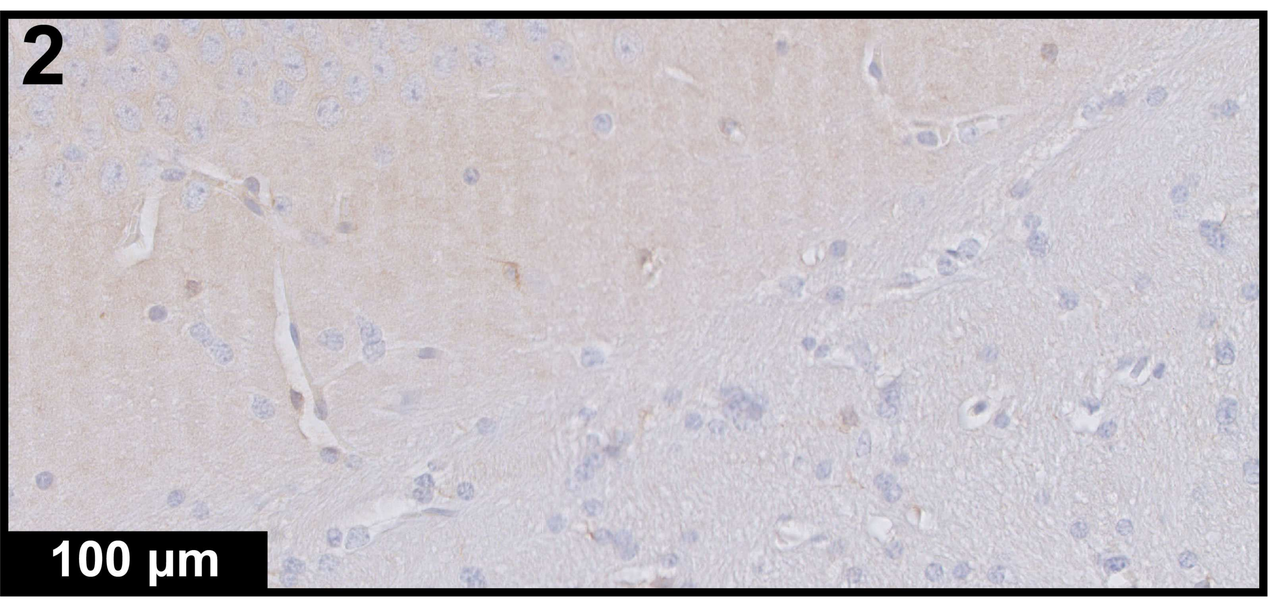

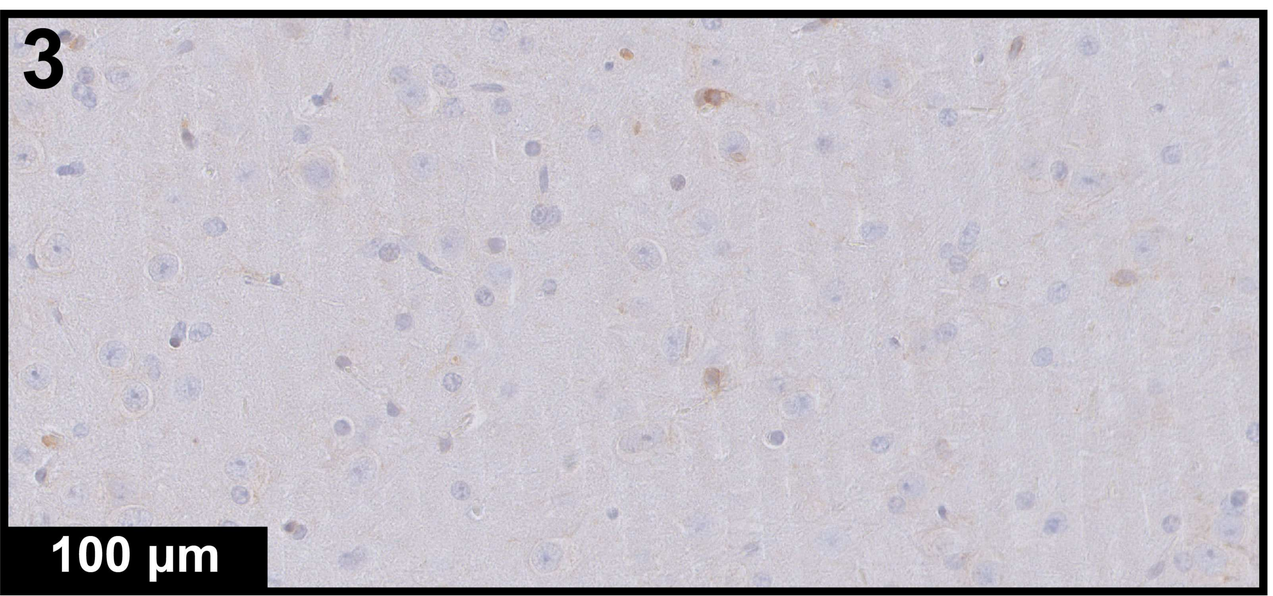

Tg-SwDI